THE ASTROPHYSICAL JOURNAL, 212:37–51, 1977 February 15

THE SPECTRUM OF THE SEYFERT GALAXY NGC 3516

A. BOKSENBERG
Department of Physics and Astronomy, University College London
AND
H. NETZER*
Department of Physics and Astronomy, Tel-Aviv University and The Wise Observatory
Received 1976 May 5; revised 1976 July 28

ABSTRACT

The Seyfert galaxy NGC 3516 was observed during 1975 using a digital image detector. Accurate measurements of emission-line intensities and profiles are presented. The narrow lines are emitted in a region with $N_e \approx 1100\ \mathrm{cm}^{-3}$. Photoionization calculations made show that excitation by a central nonthermal source can explain the observed intensity of the high-excitation forbidden lines. A cooler gas, shielded from the central ionizing source, is suggested to explain the strong [O II] and [N II] lines observed. Broad multicomponent hydrogen lines are seen in the spectrum. A decrease in the intensity of Hβ by 30% in 5 weeks has been observed and was associated with a large enhancement of Fe II broad lines near λ5270 and a change of the Hα/Hβ line ratio. Short time continuum variations can explain the change observed in emission-line intensities, provided the atmosphere is optically thick to Balmer line radiation.

Subject headings: galaxies: individual — galaxies: Seyfert

I. INTRODUCTION

Among the six galaxies originally studied by Seyfert (1943), NGC 3516 seems to have a special character because of the remarkable changes observed in its spectrum. Variations of emission-line strengths, on a time scale of 3 yr or less, were reported by Souffrin, Alloin, and Andrillat (1973) for the lines Hγ, Hβ, and [O III] λ4363.

Continuum variability also has been reported by Lyutyj (1971) and others. The variations take place mainly in the ultraviolet, as observed in other Seyfert nuclei (Penston *et al.* 1974).

The redshift measured from the emission lines indicates a distance of 50.5 Mpc ($H_0 = 55\ \mathrm{km\ s^{-1}\ Mpc^{-1}}$). At this distance 1″ corresponds to ~250 pc. As we do not have any evidence for line emission outside the nuclear region, we shall assume here that most of the emission takes place in a region 500 pc or less in diameter. The flux in the optical region, assuming the above distance, seems to be one of the largest for the galaxies listed by Seyfert (1943).

The aim of the present investigation was to obtain accurate data on emission-line intensities and profiles. We have tried to explain the emitted spectrum with the aid of a photoionization model, and to correlate the emission-line variability with physical conditions in the nucleus.

II. OBSERVATIONS AND LINE IDENTIFICATION

The nucleus of NGC 3516 was observed several times during 1975, using the University College London image photon counting system and the unit spectrograph on the Isaac Newton telescope at Herstmonceux. The system is described by Boksenberg *et al.* (1975*a*) where the standard observing technique is also given. Sky and object were monitored simultaneously, and the spectra were recorded in 1024 channels. The width of one channel was chosen to be in the range of 18–25 μm, which is thus the basic resolution unit.

The wavelength range covered by the observations is 3400–7300 Å, although, because of poor weather conditions, we could not obtain high quality results on lines in the range 3400–4200 Å. Different gratings gave a range of dispersions between 45 and 210 Å mm^{-1}. All strong lines have been observed at least once with a resolution of 1.5 Å to obtain good profiles. The apertures used for most observations were 1.″5 × 4.″8 with a projected image corresponding roughly to the width of one channel. Wavelength calibration was done by fitting a cubic curve to the wavelength/channel-number relation obtained for a comparison spectrum exposed under similar conditions.

Details of the observations are given in Table 1. We have listed there also the signal-to-noise ratio for each spectrum as calculated from the number of continuum photons in *one channel* at the central wavelength observed. Two of these spectra are shown in Figures 1–2. The internal consistency among spectra obtained on different nights suggests that errors in the spectra are accurately represented by photon statistics. This implies that a few unmarked features in the spectrum are emission lines which we could not identify.

Because of poor weather conditions, we did not attempt any absolute calibration of our measurements. (A few standard stars were indeed observed, but were

* Supported in part by the Israel Commission for Basic Research.

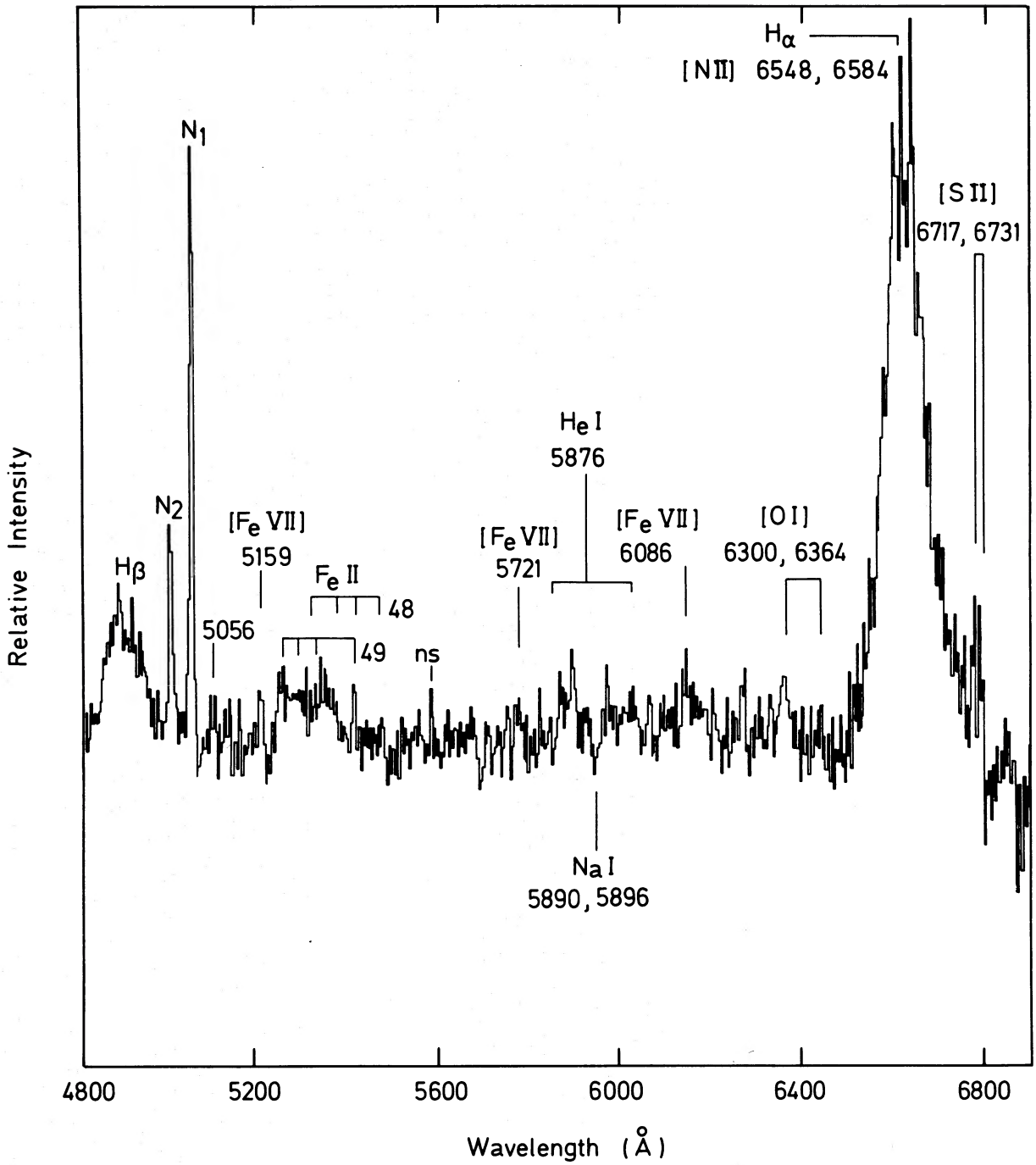

FIG. 1.—The red spectrum of NGC 3516 (original dispersion 150 Å mm^{-1})

used only for getting the continuum slope in different regions.) Instead we have used photoelectric observations of NGC 3516 obtained by M. V. Penston on the 5 m Hale telescope during 1971. One such observation is described by Boksenberg *et al.* (1975*a*), and a few more were kindly given to us by M. V. Penston. The scans were obtained through 5″, 10″, and 20″ apertures, centered on the nucleus, and one through a 5″ aperture 10″ north of the nucleus. We have chosen the 5″ aperture observation as representing our observed continuum and have calculated relative line strengths using measured equivalent widths of our spectra. Possible changes of the continuum slope are probably not important for $\lambda > 4500$ Å. This can be checked by

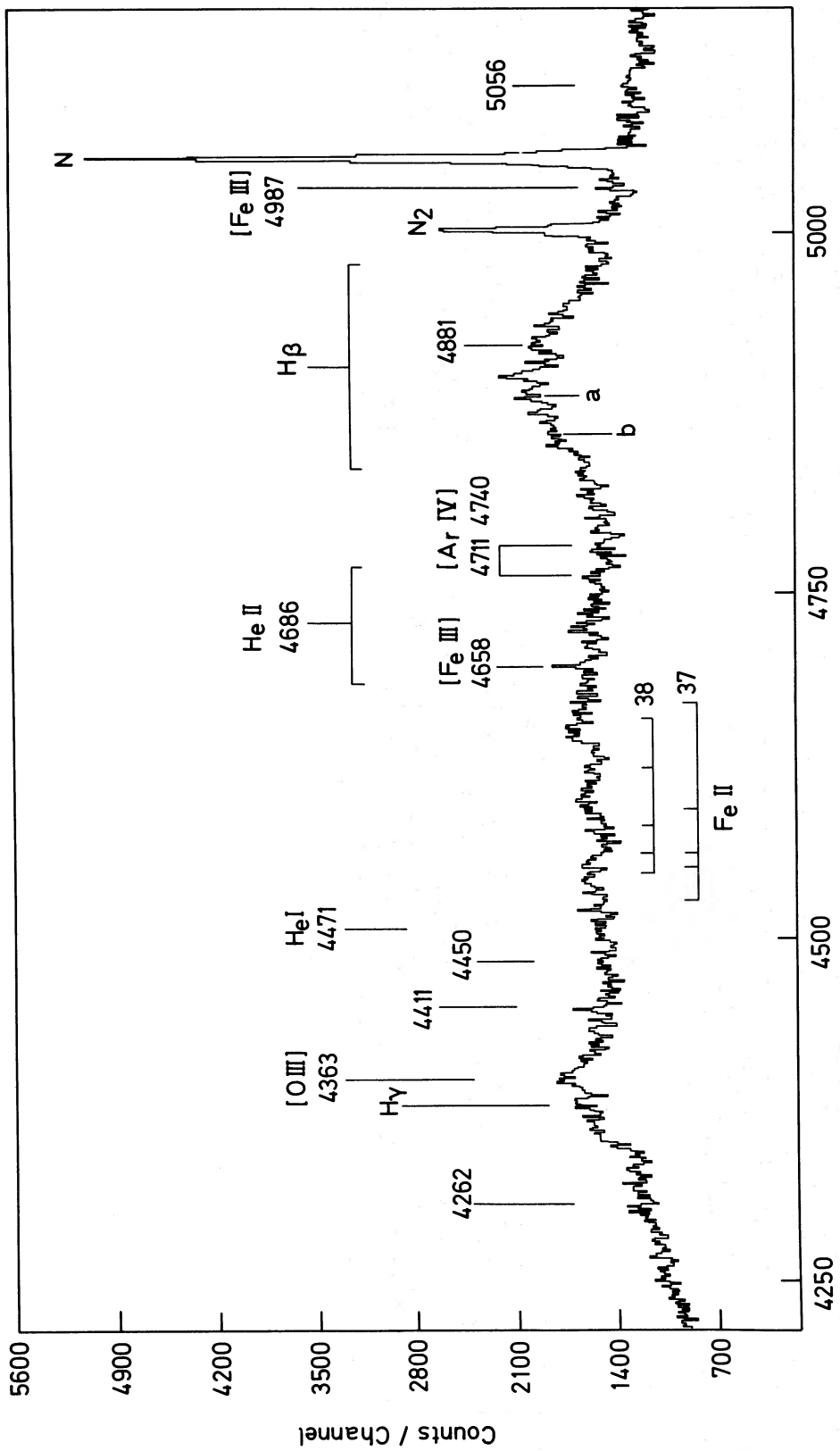

FIG. 2.—The blue spectrum of NGC 3516 (original dispersion 45 Å mm^{-1})

comparing the equivalent width and intensity of a certain line with results of other observers. We have compared the intensity of the strong [O III] lines at λ5007 and λ4959 with the measurements of Anderson (1970) and Souffrin, Alloin, and Andrillat (1973). While we have strong evidence for ultraviolet continuum changes between our observations and the ones mentioned above, we find very good agreement for the intensity of these lines in all cases. (The line strength was calculated by the above authors also using its measured equivalent width.) We conclude that no appreciable change of the continuum has occurred since 1970 for $\lambda \geq 4900$ Å. We shall discuss this point further in §§ III and V.

The general appearance of the spectrum is typical of many Seyfert galaxies. Narrow forbidden lines (~ 500 km s^{-1} FWHM) and extremely broad permitted hydrogen lines (~ 5000 km s^{-1} FWHM and $\sim 11{,}000$ km s^{-1} at the continuum level) are seen. The broad Hα and Hβ show multicomponent structure which can be interpreted as emission from several distinct clouds. We shall use the general assumption made in such cases (see, for instance, Netzer 1976) that the forbidden lines are formed in a low-density region, while the permitted lines come from a region of high internal motion and density high enough to suppress the forbidden lines. We can clearly identify the narrow component of Hβ, superposed on the broad line shown in Figure 2. This narrow component comes presumably from Hβ emission in the narrow line region.

Another feature characteristic of many other Seyferts is the appearance of both low-excitation (e.g., [O I] λ6300) and high-excitation (e.g., [Ne V] λ3426) lines in the spectrum. In addition to lines already noted by other observers, we find a rich spectrum of Fe II lines, mainly around λ5300 and λ4500. These lines were first identified in NGC 3516 by Boksenberg *et al.* (1975*a*) and are known to be present in the spectrum of many Seyfert galaxies (Boksenberg *et al.* 1975*b*). We identified them with multiplets 37, 38, 48, and 49 of Fe II. The Fe II lines are much broader than the forbidden lines, and we shall assume they are formed in the high-density region.[1] Few helium lines are seen in the spectrum; He II λ4686 is quite strong and certainly broad, but the profile of He I λ5876 is less clear. As seen in Figure 1 a strong absorption feature, which we identified as Na I λ5890, λ5896 in absorption, is seen and comes presumably from an underlying stellar component. On top of that, the strong night-sky Na I line is very close to the center of the redshifted helium line, and the subtraction procedure, if not perfect, would affect this region. We think there is a broad weak He I line at λ5876, but its intensity is most unreliable. Broad He I λ4471 is seen with an intensity not far from the one calculated by Robbins (1970), assuming the value given in Table 2 for He I λ5876 intensity is correct.

[1] Although the Fe II lines occur in complex blends, there are a few which are well separated from others. For instance, the strongest line of multiplet 37 at λ4629 as seen in many peculiar stars (cf. Aller *et al.* 1973) should easily be separated if it had the width of the forbidden lines.

TABLE 1

OBSERVATIONS OF NGC 3516

Date (1975)	Dispersion (Å mm^{-1})	Wavelength Range (Å)	S/N*
February 4/5.....	210	3400–7300	33
February 7/8.....	45	4300–5200	15
March 16/17.....	150	4700–7300	25
March 16/17.....	45	4200–5200	20
April 29/30.....	45	3400–4200	14
April 30/May 1....	60	5700–7200	17
April 30/May 1....	45	4200–5300	38
April 30/May 1....	45	3400–4200	25
May 2/3.....	210	3400–7300	45

* S/N is the signal-to-noise as calculated from the number of continuum photons in one channel at the central wavelength observed.

There may be a broad component of [O III] λ4363 blended with Hγ. If this identification is correct (cf. § V), this would be the first example of a broad forbidden line in a Seyfert galaxy spectrum. A narrow component of this feature can be identified with the [O III] λ4363 line that comes from the narrow line region.

A remarkable change of the emission-line spectrum occurred during our observations. A drop of $\sim 30\%$ in Hβ and Hγ intensity, followed by a large enhancement of a few Fe II lines, was observed on a time scale of 5 weeks. Because of its prime importance for the present investigation, we shall discuss this change, with relation to other spectral changes, in a separate section.

A few absorption features are seen in the spectrum, most of them in the region of $\lambda < 4300$ Å which is not shown in either Figure 1 or Figure 2. These are all identified with strong stellar lines and presumably come from the underlying galaxy. An extensive discussion of this absorption spectrum has been given by Souffrin, Alloin, and Andrillat (1973) and others, and we shall not discuss it any further.

Relative and absolute line strengths, as measured on different spectra, are listed in Table 2. As few of the broad lines exhibit large changes in intensity, the table gives their intensity as correct for the period 1975 Feb. 4–7. (See § V for measurement on other nights.) The uncertainty involved in the intensity measurements varied according to the different wavelength range and the line strength. Strong lines such as [O III] λ5007 have not shown intensity differences larger than 5% on two different occasions, but the uncertainty in measuring weaker lines is higher. We believe our measurements of lines having $\lambda > 4500$ Å are accurate to about $\pm 30\%$, although the measurement of the [S II] lines may only be accurate to $\pm 50\%$. Lines having $\lambda < 4500$ Å seem to be less reliable because of the lower quality of observations there and a possible systematic error in continuum fitting. The uncertainty involved in the intensity of [O II] λ3727 and [Ne V] λ3425 may be as large as a factor of 2. (This seems to be pessimistic as the agreement with Anderson's 1970 observations for these lines is quite satisfactory.) The intensities mea-

TABLE 2

EMISSION-LINE INTENSITIES IN NGC 3516

λ_0 (Å)	Identification	Flux (10^{-14} ergs s^{-1} cm^{-2})	Relative Intensity
3426	[Ne v]	7	5.6
3727	[O II]	7.5	6
3868	[Ne III]	4.1	3.3
4070	[S II]	$\leq$1.2	$\leq$1
4101	Hδ core + wings	23.7	19
4340	Hγ core + wings	40	32
4363	[O III] core + wings	21.2	17
4412	[Fe II]?	3.7	3
4471	He I	6.2	5
4490–4630	Fe II multiplets 37, 38	$\lesssim$87	$\lesssim$70
4658	[Fe III]	2.5	2
4686	He II core + wings	26.2	21
4711	[Ar IV]	2.5	2
4740	[Ar IV]	2	1.6
4861	Hβ core	3.7	3
	Hβ wings	121.2	97
4881	[Fe III]?	$\leq$1.2	$\leq$1
4959	[O III]	15.6	12.5
5007	[O III]	47.5	38
5056	?	$\leq$3.7	$\leq$3
5158	[Fe VII]	$\leq$3.7	$\leq$3
5200–5360	Fe II multiplets 48, 49 [Ca V] 5309?	32.5	2.6
5721	[Fe VII]	9	7.2
5876	He I core + wings	$\leq$28.7	$\leq$23
6086	[Fe VII]	11.6	9.3
6300	[O I]	11.6	9.3
6364	[O I]	3.7	3
6548	[N II]	6.9	5.5
6563	Hα core	18.1	14.5
	Hα wings	544	435
6584	[N II]	11.9	9.5
6717	[S II]	8.5	6.8
6731	[S II]	8	6.4

sured for the broad Hα and Hβ lines are probably good to $\pm$10%, but there is much more uncertainty involved in the separation of the broad and narrow components of these lines.

III. THE CONTINUUM

A detailed discussion of the continuum spectrum of NGC 3516 is given by Souffrin, Alloin, and Andrillat (1973). These authors find, in addition to a normal spiral galaxy spectrum, a contribution from a nonstellar continuum increasing toward the ultraviolet region. The relative contribution of this component depends on the aperture used for the observation and increases toward the nucleus. According to Souffrin, Alloin, and Andrillat, 30% of the total flux at $\lambda = 4000$ Å comes from a continuum nonstellar in origin when observing the nucleus through a 7″ aperture.

To investigate this question further, we have used the scanner observations obtained by M. V. Penston, for which the nucleus flux was observed through different apertures. The wavelength region covered by these observations is 3260–11200 Å with a resolution of 40 Å in the blue and 80 Å in the red part of the spectrum. We have used observations made on the same night and have subtracted the flux observed through different apertures to obtain the underlying stellar continuum. This was done for the 20″ − 10″ and 10″ − 5″ aperture combinations and together with the continuum observation made 10″ north of the nucleus gives the stellar continuum shape in three different regions at approximately 3.5″, 8″, and 10″ away from the center. The error associated with the

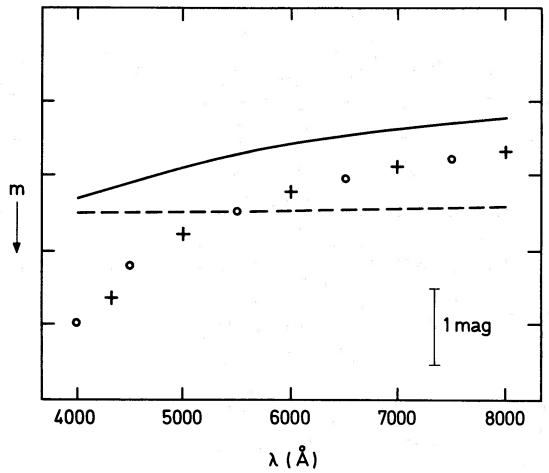

FIG. 3.—Different components in the continuum of NGC 3516: $m = -2.5 \log f_\nu$; ———, observed continuum (5″ aperture); — — —, calculated nonthermal contribution (see text); + + +, calculated stellar contribution (see text); ○ ○, observed underlying galaxy (obtained by subtraction 10″ − 5″ apertures).

subtraction procedure is large, but we found that the continuum shape for $\lambda \geq 4000$ Å can reliably be obtained using this method. Figure 3 displays the observed continuum and the stellar component deduced in this way.

The technique described above was first applied to Seyfert nuclei by Wampler (1971), who obtained the stellar continua near the nuclei of NGC 1275, NGC 7469, and NGC 1068. The continuum we find for the three different regions is similar to the ones found by Wampler for the three galaxies he observed, and resembles also the continua of M51 and M32 as shown by him.

The procedure described here is associated with three major difficulties:

1. Effects of seeing and differential refraction can be a severe problem, especially at short wavelengths and when using a small aperture. This is fully discussed by Penston and Penston (1973) where a correction procedure also is suggested. The minimum zenith distance of NGC 3516, as observed from Mount Palomar, is $\sim 40°$, and the effects mentioned can alter our results considerably.
2. The stellar population itself may change with distance from the center.
3. A possible Balmer jump prevents the fitting for $\lambda \lesssim 3700$ Å.

It was not considered practical to correct for effect (1), and we have used only the wavelength range 4300–8000 Å for continuum fitting. The great similarity in shape between the underlying stellar continuum as found by the subtraction procedure and the total flux observed through a 5″ aperture for $\lambda \geq 6000$ Å may suggest that any nonstellar contribution to the continuum there must be small. Taking a nonstellar contribution of 5% for $\lambda \geq 6000$ Å, and fitting the continuum observed at this wavelength range to the stellar one we calculated, we find a *rise* of the extra nonstellar component toward shorter wavelengths, nearly linear in λ^{-2}. This is rather unusual and does not resemble any nonstellar continuum known from observations of other Seyfert galaxies.

It is possible to invoke a different, nearly flat nonthermal continuum, which will explain both the stellar-like continuum at $\lambda \geq 6000$ Å and the total flux for $\lambda \leq 6000$ Å. Such a continuum having a shape of $F_\nu \propto \nu^{-0.1}$ is shown in Figure 3. As seen from the diagram, the nonthermal contribution at $\lambda = 6000$ Å is nearly 30% of the total flux, but the overall shape can nicely be explained as a combination of the flat nonthermal continuum and a stellar contribution similar to the one we have observed, although this gives a slightly stronger continuum than observed for $\lambda \lesssim 3700$ Å.

Two additional pieces of information can be used. The first is the change in the *U* band of the continuum, observed by Lyutyj (1971) and others, while no report on a change in the *V* band is known to us. Second, one can check the continuum slope for variability, as was done by Souffrin, Alloin, and Andrillat (1973). We find no appreciable change of slope for $\lambda \geq 4500$ in any observation published so far (allowing for changes in the different apertures used). As few of the observations reported by Souffrin, Alloin, and Andrillat were done during large changes in emission-lines flux, which we believe is correlated with the continuum variation (see § V and also Cherepaschuk and Lyutyj 1973 for possible correlation between Hα and *U* band variability), we conclude that the varying component does not change by more than ~0.1 mag at λ5000. This limits the possible change of the nonthermal source shown in Figure 3 to a maximum of about 0.3 mag. The equivalent width of [O III] lines at λ4959 and λ5007 can be used as an independent test for continuum variability. These lines are coming from a large region (see discussion in § IV) and cannot suffer a large intensity change on a short time scale. We have measured their equivalent width on two different occasions, during which a change of ~30% has occurred in the intensity of Hβ, and have found no change within the observational uncertainties (~10%).

On the basis of the above, we suggest that the nonthermal component shown in Figure 3 has the right shape, but it is too strong by about 30%. In such a case an additional contribution is necessary to explain the extra emission in the ultraviolet. This may come from hot blue stars in the nuclear bulge, similar to the situation found in normal spiral nuclei (Osterbrock 1970).

In what follows we assume two possible nonthermal sources that may provide the ionizing flux in the nucleus of NGC 3516. One is the continuum just discussed with a flux of:

$$F_\nu = 1.2 \times 10^{28} \nu^{-0.1} \exp\left[\tfrac{1}{4}(1-\nu)\right] \text{ ergs s}^{-1}\text{ Hz}^{-1}, \quad (1)$$

where ν is the frequency in rydbergs, and the flux at the Lyman edge (1.2×10^{28} ergs s^{-1} Hz^{-1}) was calculated assuming a distance of 50.5 Mpc. The cutoff at 4 rydbergs has been introduced to fit best the observed He II 4686/Hβ ratio which depends mainly on the continuum slope (Williams 1971).

A second nonthermal continuum is given by:

$$F_\nu = 5.5 \times 10^{27} \nu^{-1.1} \exp\left[\frac{(1-\nu)}{30}\right] \text{ ergs s}^{-1}\text{ Hz}^{-1}. \quad (2)$$

This was obtained assuming 90% of the emission at λ3500 within 5″ aperture is coming from a nonthermal source, and demanding enough photons beyond the Lyman edge to explain the observed Hβ flux.

IV. THE NARROW-LINES REGION

a) Reddening

The Hα/Hβ line ratio (narrow component) calculated from Table 2 is much larger than that predicted by radiative recombination theory. Self-absorption effects can change this ratio considerably (Netzer 1975*a*), but cannot be of great importance under low-density conditions, and some other explanation must be proposed.

We assume that the steepening of the Balmer decre-

TABLE 3

OBSERVED AND CALCULATED LINE INTENSITIES

Line	Observed	Reddening Corrected	Model 1	Model 2
[S II] λ6717, 6731.....	350	190	10	50
[N II] λ6584, 6548.....	510	210	2	10
[O I] λ6300, 6364.....	420	259	293	75
[Fe VII] λ6086.....	320	210	22	18
He I λ5876.....	?	...	4.5	10
[O III] λ5007, 4959.....	1750	1640	2280	2510
Hβ.....	100	100	100	100
He II λ4686.....	?	...	29	25
[O III] λ4363.....	30*	38	22	21
[S II] λ4076, 4068.....	≤30*	≤44	0.6	2
[Ne III] λ3869, 3968....	148	246	75	85
[O II] λ3726, 3729.....	207	358	26	15
[Ne V] λ3426, 3345....	325	640	120	44

* Very unreliable.

ment is caused by reddening inside the nucleus, similar to the reddening found by Wampler (1971) in other Seyfert galaxies. Unfortunately no direct measurement is possible, as the lines usually used for this ([S II] line pairs at ~λ10300 and λ4070) are too weak to be accurately measured. We have used the observed Hα/Hβ to calculate the reddening, using the curve given by Osterbrock (1974). This is based on a reddening law similar to the one in our Galaxy. The intensities so derived for different lines are listed in Table 3.

b) Density

The relative intensity of different line pairs enables us to deduce the electron density in the narrow-line region. The best indication is given by the observed ratio of the two [S II] lines $I(\lambda6717)/I(\lambda6731) = 1.05 \pm 0.2$. These lines come from a low-excitation region, for which we take $T_e = 10{,}000$ K. Using the calculations of Saraph and Seaton (1970) we find $N_e \approx 1100\ \mathrm{cm}^{-3}$. Another observed ratio, for the [Ar IV] lines, gives $I(\lambda4740)/I(\lambda4741) = 0.8 \pm 0.2$. This gives, using the above reference, $N_e \approx 900\ \mathrm{cm}^{-3}$ if $T_e = 2 \times 10^4$ K, and $N_e \approx 1100\ \mathrm{cm}^{-3}$ if $T_e = 3 \times 10^4$ K. The temperatures mentioned are typical of the region where the high-excitation lines are formed, as we shall show later.

On the basis of the above deduction, we have taken the value of $N_e = 1100\ \mathrm{cm}^{-3}$ as representing the electron density in the narrow-line region. This value has been deduced from both low- and high-excitation lines and indicates that no large density fluctuations occur in this region. The uncertainties involved are of the order of ±25%.

c) Ionization Structure

We have carried out calculations for different photoionization models, in an attempt to explain the observed narrow-line spectrum. In each model we calculated the ionization structure of a gas filament, assuming ionization by one of the nonthermal sources described in § III. The method used for the calculations is similar to the ones of MacAlpine (1972) and Shields (1974), and was fully described by Netzer (1976). We have used the most recent cross sections available and have included charge transfer reactions for both nitrogen and oxygen. Ionization by soft X-rays and secondary electrons is also taken into account.

Following Davidson (1972) and others we introduced the variable $U_\nu \equiv F_\nu/N_e$, where F_ν is the flux measured at the cloud inner surface. For small changes of density and flux nearly all quantities of interest, like relative line intensities and ionization structure, depend on U_ν only. U_1 and U_4 are used to describe the values of U_ν and 4 rydbergs, respectively.

The gas distribution in the nucleus is not known, but evidence from Seyfert galaxies (Ulrich 1973; Walker 1968) suggests a possible configuration of a few large clouds surrounding the central source, each ~100 pc in diameter. A filling factor of 10^{-2}–10^{-3} in each cloud seems to be typical of the above two cases.

Model 1.—The ionizing continuum in this model is the one given by equation (1) in § III. Here $F_\nu \propto \nu^{-0.1}$ with a cutoff at ~4 rydbergs to give the right flux in the He II Lyman continuum. The assumed abundances of C, N, O, Ne, S, Mg, and Fe are those listed by Allen (1973). The helium abundance was assumed to be $N(\mathrm{He})/N(\mathrm{H}) = 0.06$, but this is rather arbitrary and any helium abundance close to 0.1 would be as good.

Calculations have been carried out for a gas filament situated 150 to 300 pc from the ionizing source, having constant density of $N_\mathrm{H} = 1000\ \mathrm{cm}^{-3}$. A plane-parallel geometry was chosen for the filament. The ionization structure and the run of temperature in one such cloud are shown in Figure 4.

Emission-line intensities as calculated for model 1 are listed in Table 3. The intensity is calculated by adding *equal* contributions from clouds, one at 150 pc and the other 300 pc from the ionizing source. This suits a situation in which clouds are uniformly distributed around the nucleus, covering the distance range ~100–350 pc. Comparing the observed intensity of Hβ with the flux beyond the Lyman limit, we find that in this model, 1% of the central source sky is covered by low-density clouds (~6% assuming reddening) and the

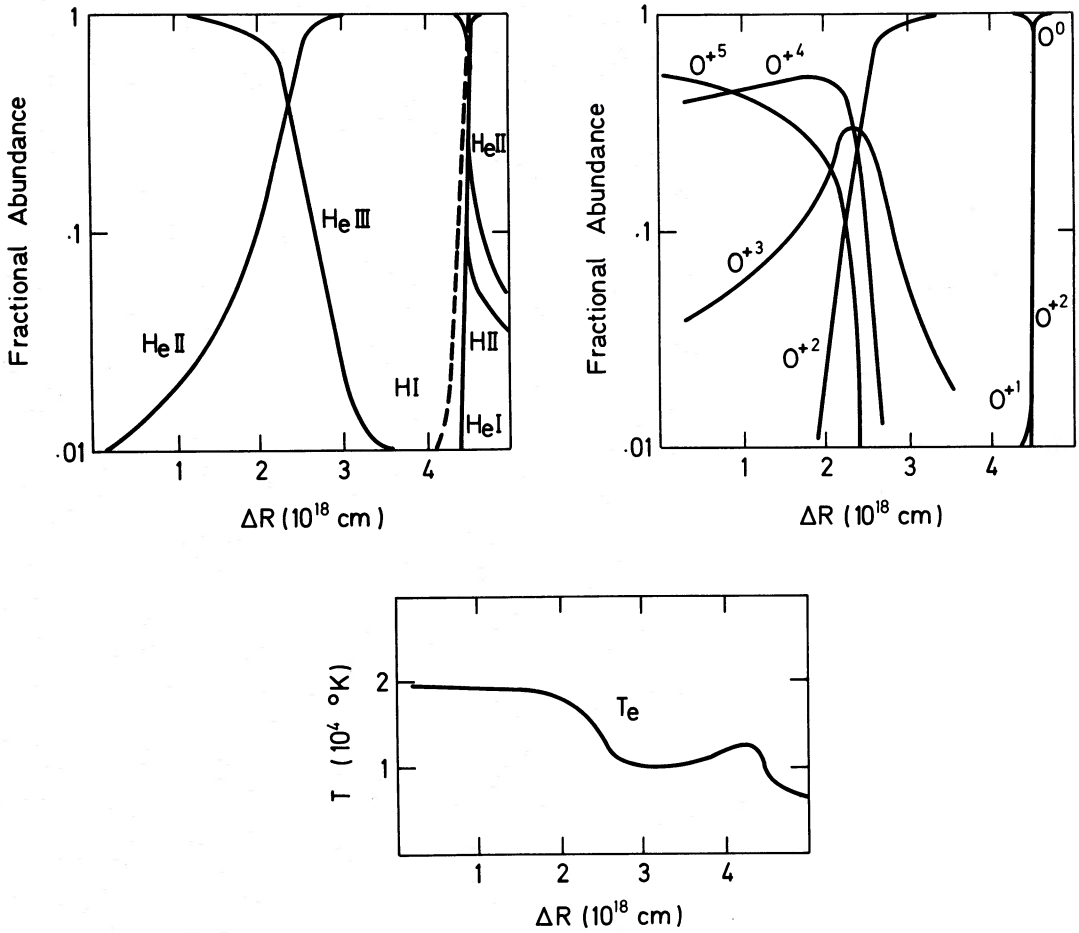

FIG. 4.—The ionization and temperature profile in model 1

ionized material mass is $\sim 10^5 M_\odot$ ($\sim 6 \times 10^5 M_\odot$ assuming reddening).

Looking at Table 3, we find that the relative strength of Hβ/([O III] λ5007 + 4959) and the lines of [O I] is predicted quite nicely for model 1. The lines of [Ne III] and [Ne V] are too weak by a factor of ~4, but [Ne III]/[Ne V] is close to the observed ratio. Large discrepancies are found for the low-excitation lines of [O II], [N II], and [S II]. It is of interest to note that when taking only one cloud at 300 pc, the agreement is much better; for instance, the relative strength of the [O I], [S II], and [N II] lines increases by a factor of ~2, while that of [O II] λ3727 increases by a factor of ~4.

Model 2.—The frequency dependence of the flux in this model is given by equation (2).

In this model, excitation of low-density material occurs only through a small fraction (~3%) of the sky which is not covered by high-density clouds. The gas is assumed to be distributed in small filaments around the center, with a filling factor of 0.01, and the limit of the H^+ region is found to be at 120 pc from the center. Heavy element abundances and total density are those of model 1, but $N(\mathrm{He})/N(\mathrm{H}) = 0.1$.

Relative line strengths, as calculated in model 2, are listed in Table 3. Somewhat better agreement with observations is found for low-excitation lines, but the high-excitation lines and the ratio $I(\mathrm{H}\beta)/I([\mathrm{O\ III}]\ \lambda 5007 + 4959)$ seem to be inferior to those of model 1.

d) Interpretation of Line Strengths

Although the shape of the ionizing continuum is not yet known, it is clear that few difficulties exist for any nonthermal continuum taken. Regarding the relative intensity of the high-excitation lines of [Ne V] and [Fe VII] the discrepancy shown in Table 3 is not large. The role of Ne^{+4} and Fe^{+6} in cooling gas is not very important, even in the high-temperature zone, and most of the differences between our calculations and observations can be attributed to uncertainty in atomic parameters and possible changes of abundances. Especially for Fe ions, the uncertainty involved in the ionization cross sections and the mixing of different ionization stages by X-ray ionization can affect the calculations considerably. (In fact we could improve the relative strength of these lines by changing U_1 and the cutoff frequency slightly from those of model 1.) Moreover, if clouds of a certain size dominate the emission region, it may well be that closer to the center the gas is optically thin (density-bounded), in which case the relative contribution of high-excitation lines

is larger. We have calculated one such model and found it to give most of the necessary missing flux in these lines.

The low-excitation lines seem to present a more severe problem, and the observed intensity of the [O II], [S II], and [N II] lines is larger by an order of magnitude than the one calculated. We have changed the cutoff frequency of model 1 in the range 1–10 rydbergs, but the problem remained basically the same. As higher-excitation lines give better agreement with observations, we conclude that, in addition to the gas excited by the nonthermal source, there must be another component which emits mainly low-excitation lines.

The problem of an additional low-excitation component in the nucleus of NGC 1068 was discussed in great detail by Shields and Oke (1975). Most of their conclusions seem to fit also the case of NGC 3516, and we shall not repeat them here but only mention briefly the more important points. One plausible explanation is that the emission comes from a gas in the shadow of an optically thick cloud. Such a model has been worked out by Van Blerkom and Arny (1972), where it was shown that a cloud ionized by the diffuse radiation of an unshielded cloud will emit mostly lines of low-excitation ions. For instance, N^0, N^+ and O^0, O^+ are the most abundant nitrogen and oxygen ions in such a region. The geometrical configuration in the nucleus of NGC 3516 suits such a model because a large fraction of the low-density gas may be shielded by clouds in the high-density region (which are much closer in and cover a large fraction of the source sky). The limitation proposed by Shields and Oke on the maximum amount of diffuse radiation expected is not valid in the case of NGC 3516 because diffuse radiation escaping from high-density clouds can also excite the low-density gas.

A time-dependent model also was suggested by Shields and Oke, involving a shock wave or continuum variability. This mechanism may indeed affect the observed spectrum, providing the variation is on a long enough time scale.

It is interesting to note a great similarity in relative intensities of [N II], [O II], and the Balmer lines in the narrow-line region of NGC 3516 and the spectrum of normal galaxies. In fact, a combination of $\sim 60\%$ of model 1 and $\sim 40\%$ of the spectrum of M51, a typical spiral studied by Osterbrock (1970), would be in good agreement with observations of most strong lines. We suggest that part of the narrow emission lines may come from H II regions in the nucleus excited by hot stars. These H II regions may have densities similar to the ones earlier discussed and are shielded from the central source by high-density clouds. We also suggest that the extra continuum flux which was discussed in § III comes from hot stars in such regions.

We cannot decide which of the above explanations holds for NGC 3516. On the basis of Shields and Oke's (1975) calculations, the ionization by diffuse radiation can certainly provide a good explanation, but the time-dependent model is less satisfactory. Contribution from H II regions inside the nucleus is also plausible. Ultraviolet observations of the continuum should resolve this point by showing the fractional flux which is not nonthermal in origin.

As mentioned by Shields and Oke (1975), self-absorption effects can be important in a recombining gas. Calculations we made showed that the required amount of partly ionized gas may indeed be found, assuming the continuum of model 1 and distances not exceeding 50 pc. Long time variations are needed for the time-dependent model (of the order of the recombination time, which is ~ 100 yr for the density we have assumed). Although short time variations have been reported, we do not see any significant difference between our observations and those of Seyfert in 1943. This is based on the Hβ flux which reflects the number of photons in the Lyman continuum. A continuum which was much brighter in the past is needed for this mechanism to be important. If self-absorption is important, then the reddening inside the nucleus is much smaller than earlier assumed. This question can be resolved when accurate observations of Hγ/Hβ for the narrow-line region are available (for self-absorption in a low-density gas Hγ/H$\beta > 0.5$ while for the reddening we found Hγ/H$\beta \approx 0.37$).

V. THE BROAD-LINE REGION

a) Line Profiles

The broad-line spectrum of NGC 3516 is interesting in a few respects. First, there is a broad feature at a wavelength coinciding with the [O III] λ4363 forbidden line. Second, the line profiles are certainly multicomponent and possibly indicate a multicloud structure of the emission region. This is demonstrated by the Hβ profile shown in Figure 2.

In Figure 5 we show the profile of Hα. The feature marked with *b* appears also on the Hβ profile in Figure 2. Also, the [N II] line at λ6548 is much stronger than expected (it should have $\frac{1}{3}$ the intensity of [N II] λ6584), which we attribute to a second emission feature in the Hα profile seen also in Figure 2 (marked with an *a*). Of interest are two absorption-like features immediately to the longward side of the Hβ line center (Figure 2). There are indications of these features on other spectra of the Hβ region, but a poor signal-to-noise prevents us from arriving at any definite conclusion. If indeed there are absorption lines, then we can identify them with Hβ absorption in clouds between us and the center, moving toward the center. Such absorbing clouds are seen in the spectrum of NGC 4151 (Anderson 1974) where they are moving away from the center.

The broad lines of He I and He II are weak and partly blended, and we cannot precisely define their shape. The broad Fe II lines observed seem to have a typical width slightly less than that of Hβ. Slight disagreement between the central wavelength of a few strong lines and the peak intensity of strong spectral features is indicated in Figure 2. We shall refer to this later.

The fraction of the central source sky covered by high-density clouds is $\sim 33\%$ for the model 1 continuum and $\sim 97\%$ for the model 2 continuum. These

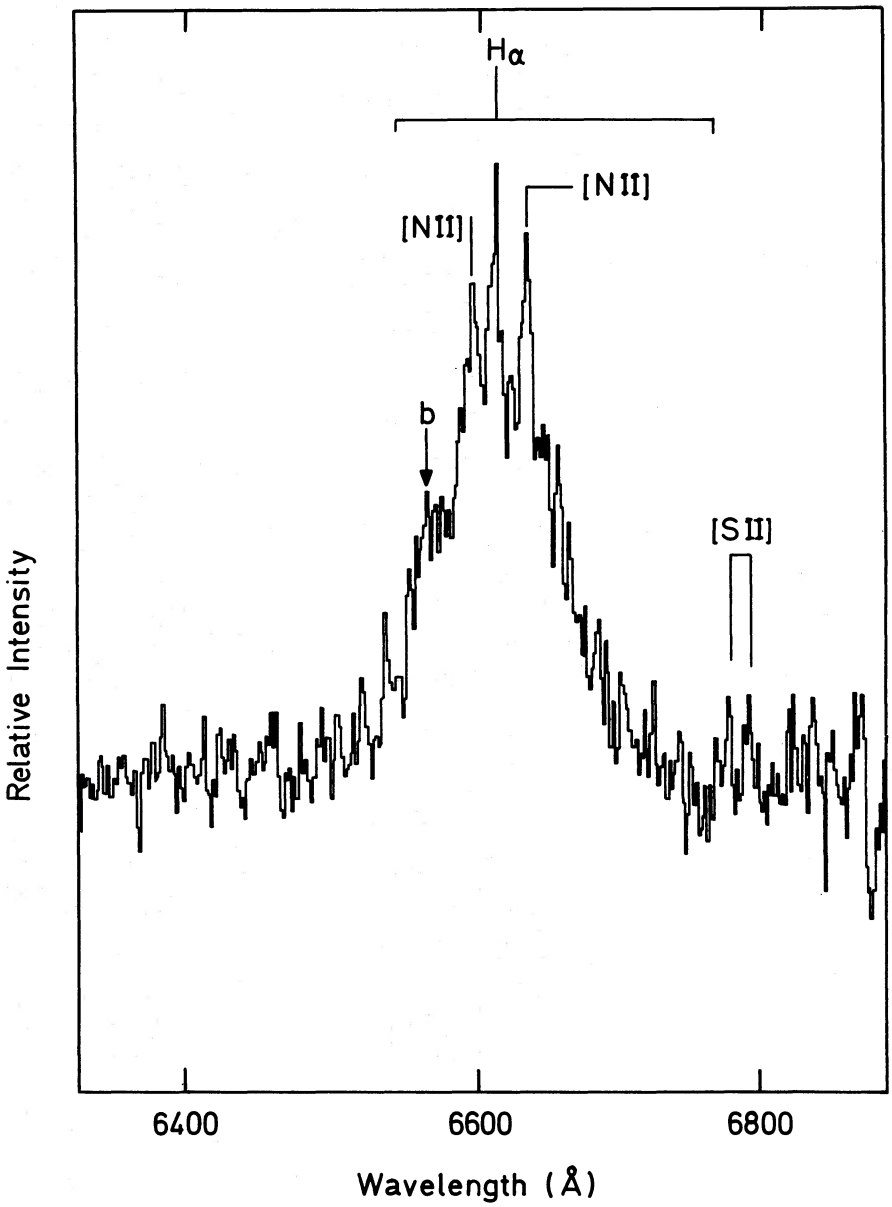

FIG. 5.—Hα region in the spectrum of NGC 3516 (original dispersion 60 Å mm^{-1}). The feature marked with *b* is identified with similar features in Hβ, shown in Figure 2.

figures are obtained when comparing the observed Hβ intensity with the one predicted by the number of photons at the Lyman continuum. The mass of ionized gas, estimated from the Hβ intensity, is $\sim 3\,M_\odot$ (assuming $N_H \approx 10^9$ cm^{-3}).

b) Variability

Remarkable changes in the spectral appearance of NGC 3516 were reported by Souffrin, Alloin, and Andrillat (1973). An increase in intensity of Hβ by a factor of 4 and a drop by a factor of ~10 for [O III] λ4363 were reported to occur on a time scale of 3 yr. Possible variations on a time scale of 1 month were also suggested.

We have observed similar spectral changes during 1975. A drop of 30% in Hβ intensity has occurred between the two observing runs of 1975 February 7 and March 16. A similar drop was noted in the intensity of Hγ + [O III] λ4363, but only ~7% drop in Hα intensity. In addition, we observed an increase by a factor of 2 in the intensity of the broad Fe II feature around λ5270 and a smaller one (which we cannot measure accurately) in the intensity of lines from multiplets 37 and 38 of Fe$^+$. The spectrum had resumed most of its February 7 appearance on May 1. The

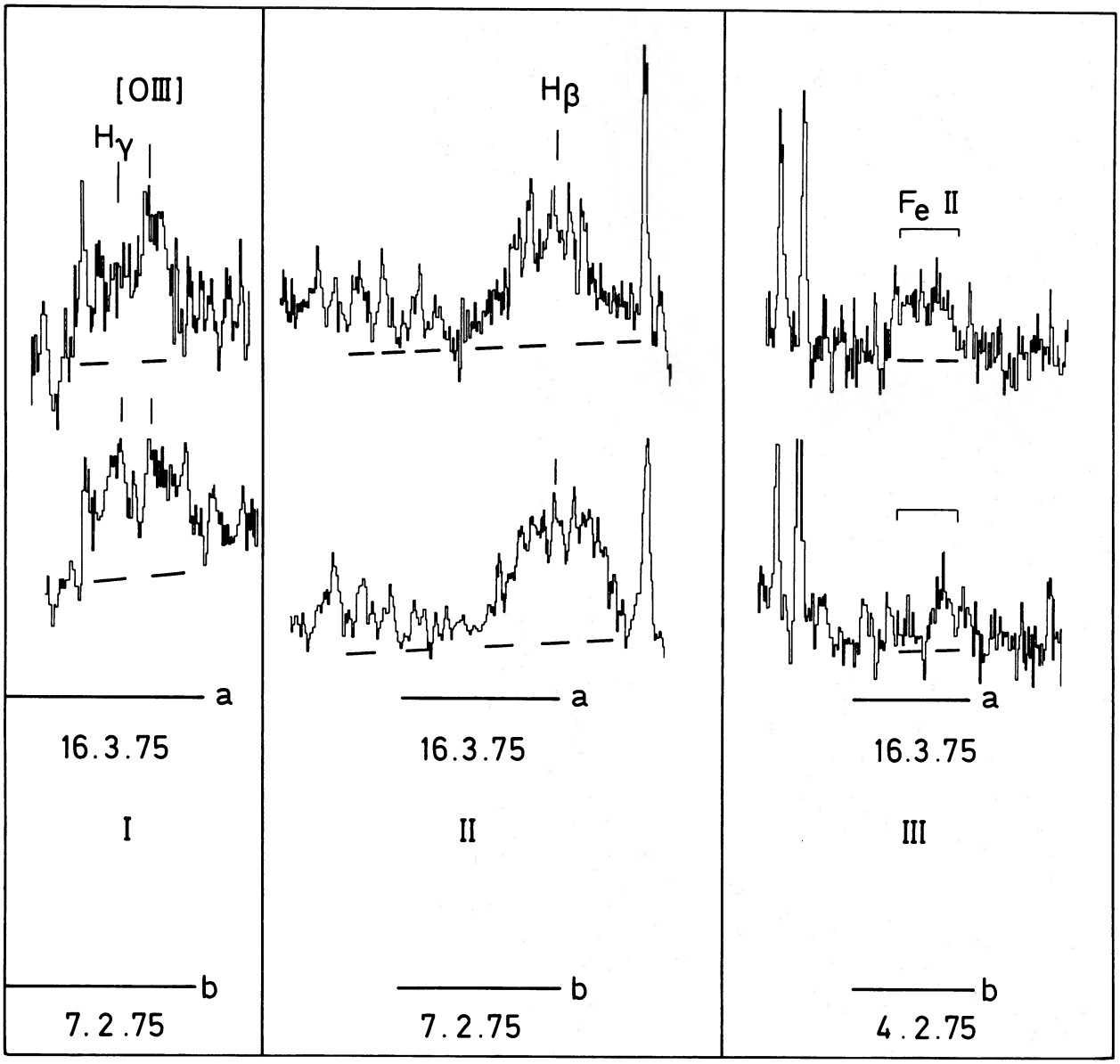

FIG. 6.—Emission-line variations observed in the spectrum of NGC 3516. The Hβ profile shown is slightly smoothed, to bring the two observations to the same signal-to-noise. Zero levels for the two spectra are indicated by *a* and *b*, with dates (day, month, year).

spectral changes as observed for Hβ, Hγ, and the Fe II lines are shown in Figure 6. We have measured the equivalent width of [O III] λ5007 on the three different occasions and found it nearly identical. This eliminates the possibility of continuum changes as causing part of the above effect. The variation observed, on a time scale of 5 weeks, puts an upper limit on the overall size of the broad emission-lines region. About one-third of the emitting gas must be within $\sim 5 \times 10^{16}$ cm from the central source, according to our observations, assuming the change is caused by continuum variability.

Of special interest are the changes observed in the Hα/Hβ line ratio. Under radiative recombination conditions we would expect this ratio to remain constant. It has, however, increased by ~30% between February 7 and March 16. We estimate the observational uncertainty involved in the measurement of this ratio to be of the order of 10%. Systematic errors, due to difficulties in continuum fitting, cannot be large, as already discussed. A list of Balmer line intensities as observed by different observers is given in Table 4. Fluctuations by a factor of ~4 are seen in the intensity of Hβ while the [O III] lines of λ5007 and λ4959 remain constant. The decrease in Hγ intensity we observed is larger than the one found for Hβ if we assume that a third of the total flux in the Hγ + [O III] λ4363 feature

TABLE 4

EMISSION-LINE FLUX IN NGC 3516 (units of 10^{-13} ergs s^{-1} cm^{-2}) AS MEASURED BY DIFFERENT OBSERVERS

Reference	Date	[O III] λ5007 + λ4959	Hβ	Hα/Hβ	Fe II λ5270
Souffrin *et al.*	1967	7.2	~2.9		
Souffrin *et al.*	1970	6.1	11.5		
Anderson	1970	6.2	3.3	5.06	
Adams and Weedman	1974	5.75	5.37	6.31	
This work	1975 Feb. 4–7	6.3	12.1	4.5	3.2
This work	1975 Mar. 16	6.3	8.9	5.8	7.1

on February 7 was due to [O III] λ4363. The *overall* decrease in flux of the Hγ + [O III] λ4363 feature is similar to the one seen in Hβ. Variations of the Hα/Hβ ratio are indicated in Table 4. Although differences between different observers may explain part of these variations, it seems that they cannot explain the change from 4.5 to 5.8 observed by us.

The Balmer decrement observed in the broad-line region resembles the one seen in the narrow-line region, and it may be proposed that it is affected by reddening in the same way. Assuming a reddening law similar to the one in our Galaxy, we find that the observed Hβ is roughly six times weaker than its unreddened intensity. This implies too bright an Hβ for any possible excitation source even when assuming a flat continuum up to 4 rydbergs (where it must drop rapidly in order to satisfy the observed He II λ4686/Hβ ratio as already mentioned) emitting 99% of the flux observed at 3500 Å. A continuum reddened itself demands a strong flux increase toward the ultraviolet which we do not regard as reasonable. It seems that the broad lines observed cannot be affected much by reddening, and a different explanation for the steep Balmer decrement must be invoked.

c) [O III] λ4363

The profile of the emission feature at 4363 Å is much broader than those of the [O III] lines at 5007 and 4959 Å. The feature has been identified as [O III] λ4363 by Souffrin, Alloin, and Andrillat (1973) who report its variation by a factor of 10 or more, on a time scale of 3 yr (and possibly 1 month). The variability reported by these authors is based upon comparison of the Hγ + [O III] λ4363 feature observed on two different occasions. We note that Figures 1*a* and 1*b* of Souffrin, Alloin, and Andrillat are almost identical to our Figure 6 (I*a* and I*b*). We can clearly see that what Souffrin, Alloin, and Andrillat have attributed to a drop in intensity of the [O III] λ4363 may well be a change in the profile of Hγ (enhancement of its blue wing relative to its red). Figure 1*c* of Souffrin, Alloin, and Andrillat and our Figure 2 may represent an intermediate stage between those two extreme situations. If this hypothesis is correct, then the central wavelength of Hγ corresponds to the center of the varying wing, and we could postulate that only weak narrow [O III] λ4363 is seen which does not vary at all. The changes observed in the profile of Hβ (Fig. 6 [II]) may indicate a similar tendency, but in any case Hγ and Hβ have different profiles.

If a broad [O III] λ4363 line does appear on the spectrum, then it must come from a high-density region in which the other [O III] lines are suppressed. We have tried to detect broad wings on other [O III] lines in order to establish this identification. Looking at Figure 2, we note a possible broadening at a level of 3 σ above the continuum adjacent to the [O II] lines at λ4959 and λ5007. This is found also on another spectrum but is even less reliable there. Assuming these features are broad components of the [O III] lines, we can put a limit of

$$\frac{I(\lambda 5007 + \lambda 4959 \text{ broad component})}{I(\lambda 4363 \text{ broad component})} \leq 0.4 .$$

The uncertainty here is large, and the ratio may be as small as 0.1. Assuming this upper limit and using Seaton's (1975) calculations for $T_e = 2 \times 10^4$ K, we find $N_e \gtrsim 10^8$ cm^{-3}. A minimum temperature in which this ratio can still exist is $T_e = 1.7 \times 10^4$ K, and this demands $N_e \gtrsim 10^9$ cm^{-3}. Such high densities are found in the broad-line region of other Seyfert nuclei (Netzer 1976), but in no case has a broad [O III] line been observed. If the [O III] line ratio is closer to 0.1, which may well be the case, then there is *no value* of N_e, T_e which can explain it and still be consistent with observations of other broad lines or excitation by any plausible nonthermal source.

The absolute intensity of [O III] λ4363 puts some severe limitations on the ionization structure. We can compare it with the intensity of the broad Hβ line through

$$\frac{I([\text{O III}]\ \lambda 4363)}{I(\text{H}\beta)} = \int_v \frac{N(^1S_0)}{N(\text{O}^{++})} \frac{N(\text{O}^{++})}{N(\text{H}^+)} \frac{4861}{4363} \frac{A_{32}}{\alpha_{\text{eff}}(T) N_e} dV , \quad (3)$$

where $A_{32} = 1.68\ s^{-1}$ is the Einstein coefficient for the $^1S_0$–$^1D_2$ transition, and $\alpha_{\text{eff}}(T)$ is the effective recombination coefficient for Hβ. As mentioned earlier, the densities under discussion are of the order of 10^8 cm^{-3} or more, and for all practical purposes we can assume local thermodynamic equilibrium (LTE) for the O^{++} levels. (The critical density for de-excitation of the $^1S_0$ state is $\sim 3 \times 10^7$ cm^{-3} if $T_e = 20{,}000$ K.) Under these

conditions we find:

$$\frac{I([\text{O III}]\ \lambda 4363)}{I(\text{H}\beta)} = \frac{1.5 \times 10^{11}}{N_e}\frac{N(\text{O}^{++})}{N(\text{H}^{+})} T_e = 1.5 \times 10^4\ \text{K}$$

$$= \frac{5.1 \times 10^{11}}{N_e}\frac{N(\text{O}^{++})}{N(\text{H}^{+})} T_e = 2 \times 10^4\ \text{K}$$

$$= \frac{1.9 \times 10^{12}}{N_e}\frac{N(\text{O}^{++})}{N(\text{H}^{+})} T_e = 3 \times 10^4\ \text{K}. \quad (4)$$

Assuming $N(\text{O})/N(\text{H}) = 6.6 \times 10^{-4}$ and all the oxygen is O^{++} throughout the H^{+} layer, we need $T_e \gtrsim 2 \times 10^4$ K if $N_e \approx 2 \times 10^9\ \text{cm}^{-3}$, and $T_e \gtrsim 3 \times 10^4$ K if $N_e \approx 7 \times 10^9\ \text{cm}^{-3}$, to explain the observed $I([\text{O III}]\ \lambda 4363)/I(\text{H}\beta)$ ratio.

The high temperature needed to explain the observed lines demands large values of U_1 and U_4/U_1. A flat continuum can give the high temperature, but most of the oxygen in the high-temperature region will be more than twice ionized. A large U_1 and cutoff around 2 rydbergs can produce a gas in which no ionization stages higher than O^{++} will exist, but the high-temperature region will be very small, and most of the $\text{H}\beta$ emission will take place under lower temperature conditions. We have tried several photoionization models for explaining such line ratios. Different possibilities of different U_1 and U_4 were tested, beside the standard models 1 and 2 of § IV. In all cases where $I(\lambda 4363)/I(\lambda 5007 + \lambda 4959) \geq 3$ we found that

$$I(\lambda 4363)/I(\text{H}\beta) < 0.05\,.$$

Only for $I(\lambda 4363)/I(\lambda 5007 + \lambda 4959) \approx 1.5$ did we have $I(\lambda 4363)/I(\text{H}\beta) \approx 0.1$. It seems that no combination can satisfy both conditions, and the ionization structure of a high-density gas cloud, ionized by a nonthermal source, does not support the observations of a strong [O III] λ4363 line.

We conclude that the features observed at λ4363 cannot all be attributed to the [O III] line, and most of it is Hγ coming from another cloud. This cloud does not share the large intensity variations exhibited by other clouds. This also involves variations of $\text{H}\gamma/\text{H}\beta$ which are probably related to the change of $\text{H}\alpha/\text{H}\beta$ shown in Table 4.

d) The Balmer Lines

The large change which occurred in Balmer line intensities can be explained by continuum variation. A change of the ionizing flux will cause such variation to appear, provided the emission region is small enough and the density there high enough to give a short recombination time. Possible correlation between Hα and U variations found by Cherepaschuk and Lyutyj (1973) tend to indicate the same. (The delay of 15–30 days between the U and Hα variations found by these authors is on the same time scale as the change observed by us, and indicates the same size for the emission region.)

Possible variations in Balmer line ratios are discussed by Netzer (1976). There it is shown that a mechanism capable of explaining such changes is self-absorption in Balmer lines. This mechanism can also produce a steep Balmer decrement (Netzer 1975*a*), which could explain the hydrogen line intensities in the spectrum of NGC 3516.

We assume now that self-absorption conditions exist in the high-density clouds close to the central source. The optical depth in Hα, under these conditions, depends only on the distance from the ionizing source (Netzer 1976). A critical distance for which this effect is important [i.e., $\tau(\text{H}\alpha) \gtrsim 50$] is $\sim 2.5 \times 10^{17}$ cm and $\sim 1.5 \times 10^{17}$ cm for the continua of models 1 and 2 of § IV, respectively. We assume about a third of the emitting gas is located inside this boundary, and the rest is found $\sim 10^{18}$ cm from the center and emits Balmer lines with a decrement close to the one predicted by radiative recombination theory. The dimensions deduced earlier for the emission region, from the short (5 weeks) and long (~4 yr) time variations, fit into this picture.

Consider a cloud R cm from a continuum source emitting F_ν ionizing photons. The optical depth in Hα is given by $\tau(\text{H}\alpha) = cF_\nu/R^2$, where c is constant for all practical purposes. The $\text{H}\alpha/\text{H}\beta$ line ratio depends on $\tau(\text{H}\alpha)$ in a functional way, which we call g. The behavior of g under different N_e, T_e conditions is described by Netzer (1975*a*, 1976). We can use the calculated ratio $\text{H}\alpha/\text{H}\beta = g(cF_\nu/R^2, T_e, N_e)$ to derive the intensity of Hα and Hβ during the continuum flux changes. Results of such calculations are shown in

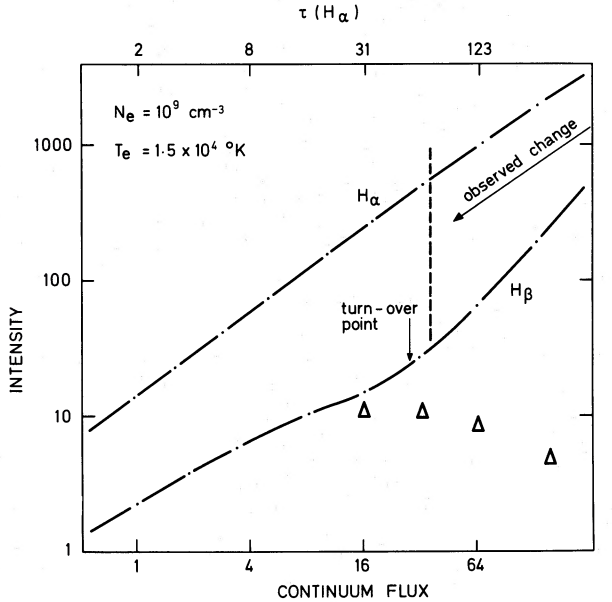

FIG. 7.—Calculated intensity of Hα and Hβ in a gas optically thick to Balmer line photons. Continuum flux is given in arbitrary units. ΔΔΔ, numerical calculations of collisionally excited Fe II lines, given on the same intensity scale as Hα and Hβ. (Results are given for the Fe II band at λ5270 Å.) The region to the right of the dashed line is where the observed change in $\text{H}\alpha/\text{H}\beta$ has taken place.

Figure 7. We have chosen $T_e = 15{,}000$ K to represent the temperature in the region where most of the Balmer line emission takes place. The density chosen, 10^9 cm^{-3}, is less important, and practically identical results would appear for N_e different by a factor of 5.

It is clear from Figure 7 that the Hα/Hβ ratio changes in a different way on different parts of the diagram. The turnover point marked is where steep decrements are starting to appear. [This is at $\tau(\mathrm{H}\alpha) \approx 60$ for the case chosen.] The part of the diagram in which a continuum flux drop would result in a *rise* in Hα/Hβ is also marked. This is similar to what we observed in the spectrum of NGC 3516. Taking one numerical example, we calculated a situation in which a third of the gas is inside the self-absorption boundary, and suffers a continuum flux drop by a factor of 4. The rest of the gas is outside this region, and not yet affected by the change. (The emission in the gas there results in Hα/Hβ = 2.7.) Taking the change to occur around the $\tau(\mathrm{H}\alpha) = 123$ point, we find an overall decrease by 30% for Hβ, 8% for Hα, and a change of Hα/Hβ from 5.1 to 7.9. This, of course, is only an example of a possible change. The real situation is more complicated, and many clouds contribute to the effect, each on a different time scale, and with different Hα/Hβ ratios defined by the values of $\tau(\mathrm{H}\alpha)$. It is, however, possible to explain in principle changes like the one observed, assuming the above mechanism.

e) *The* Fe II *Lines*

The change observed in the intensity of the Fe II band at ~λ5270 is by more than a factor of 2, and we do not know of any other galaxy where such a change has been observed. The increase of Fe II line intensities is correlated with a decrease of Balmer line strengths, a fact that ought to be explained by any model proposed.

The excitation mechanism of the Fe^+ permitted lines has been discussed by many authors. It is usually assumed that absorption of continuum radiation in resonance lines of Fe^+, around 2400 Å, is followed by cascade and reemission in the visual wavelength range. The gas must be optically thick to the resonance line photons. Calculations by Adams (1975), Netzer (1975*b*), and Osterbrock (1976) have shown that this mechanism is capable of explaining the observed intensities of these lines.

Another possible excitation is by inelastic collisions, similar to excitation of other strong lines in the spectrum. This mechanism has been compared with radiation excitation by Netzer (1975*b*) and has been shown to be more important in many situations. A large optical depth in the resonance lines is needed here also, and the efficiency depends strongly on ionization structure and temperature.

We have calculated the expected strength of the Fe II lines taking the continua of models 1 and 2 and dense close-by clouds. The lines are formed in a low-excitation H I region beyond the highly ionized H^+ layer. (We refer to this as "excited" H I region.) Such low-ionization regions have been discussed by Netzer (1976) where it was shown that they are formed whenever a considerable X-ray flux is emitted by the central nonthermal source. In such cases the penetration of high-energy photons beyond the H II layer maintains low ionization (2–8% ionized hydrogen) through ionization by He I diffuse radiation and secondary electron impacts. The temperature characterizing such a region is ~8000–10,000 K, which is high enough to excite ground level atoms of Fe^+ (the most abundant iron ion in this region). The combined thickness of the "excited" H I and the H II layers depends on the optical depth of the gas at the frequency range of 10–30 rydbergs. The main opacity in this frequency range comes about from He I and heavy-element absorption. The second of these is practically independent of ionization stage, so in many cases the total H I + H II thickness is nearly independent of U_ν. For large values of U_1 the H II is thick, and hardly any "excited" H I layer is formed. The intensity of the collisionally excited Fe^+ lines will be small in such cases. For small U_1 the "excited" H I layer can be much thicker than the H II one, and the strength of the Fe II line can exceed, according to calculations we made, that of Hβ.

Regarding the situation observed in NGC 3516, we realize that a continuum drop (which we assume was the reason for the drop in the intensity of Hβ) has resulted in a rise of Fe II line intensities. In most cases the radiation-excitation mechanism proposed earlier demands a weakening of Fe II lines during such a change (unless there is an inverse correlation between the flux at λ ~2400 Å and the flux beyond the Lyman limit, which we consider very unlikely). We propose two possible explanations for this change:

1. Most of the change observed results from emission in one cloud (or clouds in one small region, all having similar dimensions) in which the optical depth in the Fe II resonance lines, before the continuum flux drop, was small. The continuum drop has resulted in recombination of hydrogen and iron, and the optical depth in the Fe II lines has increased. Flux absorption in the lines became more efficient, and stronger lines appeared in the visual range. We have calculated one such case using the continuum of model 2. A density-bounded configuration has been assumed, and the gas cloud terminated at $\tau(\lambda 912) = 150$. The optical depth in a typical Fe II resonance line was ~3. By cutting the Lyman continuum flux to half its original intensity, the optical depth in the Fe II lines has increased to more than 1000. Such a change would result in an increase of the equivalent width of the observed Fe II lines by more than an order of magnitude (cf. Adams 1975; Netzer 1975*b*). The overall effect will be seen as a rise in the absolute line intensities by more than a factor of 5.

Such an explanation is based on a density-bounded situation, and special optical depth conditions are needed for it. Looking at Figure 6, we realize that the biggest change observed is in the blue wing of the Fe II band at λ5270. This may be correlated with the change observed in the blue wing of Hγ, assuming both to come from the same cloud. It may be that the efficiency of continuum flux absorption by Fe II atoms is different in different parts of the nucleus, which may be related to the fact that the peaks of the strongest Fe II lines around 4600 Å do not always coincide with the

strongest emission features observed in this wavelength range.

2. Collisional excitation of Fe II lines can also be suggested. As described earlier, the line ratio I(Fe II λ5270)/I(Hβ) depends on the relative size of the H II and the "excited" H I regions. The H II layer shrinks after continuum flux drop, and an increase of the above line ratio results. We have calculated the changes expected in the strength of the Fe II band near λ5270, using photoionization model calculations. The collisional excitation cross sections are not known for Fe II lines, and we can only estimate that they are not much different from those of other permitted lines. Cross sections for photoionization are taken from MacAlpine (1971). Although the accuracy of such calculations is probably not better than a factor of 2–4, they can be used to estimate the importance of the effect.

We find that for the model 2 continuum, an increase by a factor of $\sim$2 of the Fe II band around λ5270 is associated with a drop by a factor of 5 in Hβ, where, before the continuum flux drop, we take $U_1 = 4.4 \times 10^{-17}$ ergs s^{-1} cm Hz^{-1}. The ratio I(Fe II λ5270)/I(Hβ) varies from $\sim$0.04 to $\sim$0.3 during the changes. Further increase in I(Fe II λ5270)/I(Hβ) is seen when taking even smaller values of U_1, but this results only from an Hβ intensity drop, and the absolute Fe flux remains nearly constant. (The "excited" H I layer thickness is much bigger now than that of the H II, and further flux drop cannot affect much the total emission of the Fe II lines.) The numerical results obtained in these calculations are shown in Figure 7.

VI. CONCLUSIONS

We have shown that there are two region in the nucleus of NGC 3516. One region contains a low-density gas with a typical density of $N_e = 1100$ cm^{-3}, distributed in small filaments or clouds up to $\sim$300 pc from the central source. This low-density gas is excited by a nonthermal continuum situated at the center of the galaxy. We have considered two possibilities for the energy distribution of the ionized flux and have shown that in both of them the relative intensity of high-excitation lines is not far from what we observed. Low-excitation lines of [N II], [O II], and [S II] as predicted by our model seem to be in poor agreement with observations, and we suggest that a different mechanism must be introduced in order to explain their observed intensity. Shielded gas and excitation by hot stars may provide the answer for the above discrepancy.

A high-density gas having $N_e \approx 10^9$ cm^{-3} is also present in the nucleus. Judging by the recombination-line variability which we observed on a time scale of 5 weeks, we suggest that the high-density gas is concentrated 10^{17}–10^{18} cm from the ionizing source. We have found a multicomponent structure and variations in time of Hα/Hβ and few Fe II lines. We have argued that an atmosphere optically thick to Balmer line radiation and a low-excitation region in a radiation-bounded configuration can explain both these observations. Calculations we have carried out on the Fe II lines in the spectrum of NGC 3516 show that inelastic collisions may be more efficient than absorption of continuum radiation in exciting the lines.

We are grateful to the Large Telescope Users Panel for generous allocation of telescope time. We would like to thank M. V. Penston for permitting the use of his photoelectric observations of NGC 3516, and K. Shortridge, S. A. Briggs, and P. Johnson for invaluable assistance in observations and data reduction. We are indebted to the Science Research Council for financial support.

REFERENCES

Adams, T. F. 1975, *Ap. J.*, **196**, 675.
Adams, T. F., and Weedman, D. W. 1975, *Ap. J.*, **199**, 19.
Allen, C. W. 1973, *Astrophysical Quantities* (3d ed.; London: Athlone), p. 31.
Aller, L. A., Polidan, R. S., Rhodes, E. J., Jr., and Wares, G. W. 1973, *Ap. Space Sci.*, **20**, 93.
Anderson, K. S. 1970, *Ap. J.*, **162**, 743.
———. 1974, *Ap. J.*, **189**, 195.
Boksenberg, A., Shortridge, K., Fosbury, R. A. E., Penston, M. V., and Savage, A. 1975*a*, *M.N.R.A.S.*, **172**, 289.
Boksenberg, A., Shortridge, K., Allen, D. A., Fosbury, R. A. E., Penston, M. V., and Savage, A. 1975*b*, *M.N.R.A.S.*, **173**, 381.
Cherepaschuk, A. M., and Lyutyj, V. M. 1973, *Ap. Letters*, **13**, 165.
Davidson, K. 1972, *Ap. J.*, **171**, 213.
Lyutyj, V. M. 1971, *Astr. Circ. USSR*, No. 620.
MacAlpine, G. M. 1971, Ph.D. thesis, University of Wisconsin.
———. 1972, *Ap. J.*, **175**, 11.
Netzer, H. 1975*a*, *M.N.R.A.S.*, **171**, 395.
———. 1975*b*, Ph.D. thesis, University of Sussex.
———. 1976, submitted to *M.N.R.A.S.*
Osterbrock, D. E. 1970, in *Nuclei of Galaxies*, ed. D. J. K. O'Connell (Vatican: Pontificiae Accademiae Scientiaruno Scripta Varia), p. 151.
Osterbrock, D. E. 1974, *Astrophysics of Gaseous Nebulae* (San Francisco: Freeman), p. 171.
———. 1976, *Ap. J.*, **203**, 329.
Penston, M. V., and Penston, M. J. 1973, *M.N.R.A.S.*, **162**, 109.
Penston, M. V., Penston, M. J., Selmes, R. A., Becklin, E. E., and Neugebauer, G. 1974, *M.N.R.A.S.*, **169**, 357.
Robbins, R. R. 1970, *Ap. J.*, **160**, 519.
Saraph, H. E., and Seaton, M. J. 1970, *M.N.R.A.S.*, **148**, 367.
Seaton, M. J. 1975, *M.N.R.A.S.*, **170**, 475.
Seyfert, C. 1943, *Ap. J.*, **97**, 28.
Shields, G. A. 1974, *Ap. J.*, **191**, 309.
Shields, G. A., and Oke, J. B. 1975, *Ap. J.*, **197**, 5.
Souffrin, S. C., Alloin, D., and Andrillat, Y. 1973, *Astr. Ap.*, **22**, 343.
Ulrich, M.-H. J. 1973, *Ap. J.*, **181**, 51.
Van Blerkom, D., and Arny, T. 1972, *M.N.R.A.S.*, **156**, 91.
Walker, M. 1968, *Ap. J.*, **151**, 71.
Wampler, E. J. 1971, *Ap. J.*, **164**, 1.
Williams, R. E. 1971, *Ap. J.* (*Letters*), **167**, L27.

A. Boksenberg: Dept. of Physics and Astronomy, University College London, Gower St., London WC1E 6BT, England

H. Netzer: Dept. of Physics and Astronomy, Tel-Aviv University, Ramat Aviv, Israel